J Therm Anal Calorim (2011) 105:897–906
DOI 10.1007/s10973-010-1221-y

Few introducing comments on the thermal analysis of organoclays

Shmuel Yariv · Mikhail Borisover · Isaak Lapides

ESTAC2010 Conference Special Issue

Abstract Organoclays are the adsorption products of organic matter by clay minerals. In modern technology, organoclay-based nanocomposites obtained by modifying Na-clay by primary adsorption of organic ammonium cations or long-chain cationic surfactants are widely used in different industries. They are potential candidates for serving as sorbents of different organic compounds by secondary adsorption. Organoclays are widely spread in the environment and are responsible for the colloid behavior of different environmental elements such as soils. This manuscript summarizes some of the basic knowledge on thermal analysis of organoclays and reviews some of the recent studies carried out in our laboratory on organoclays which occur in the environment, those applied in industry and of those obtained by secondary adsorption processes. Complexes in the environment or those used in industry are mainly of the smectite clay mineral montmorillonite and their thermal analysis in air is treated here.

Keywords Adsorption primary and secondary · Adsorptive clays · Charcoal · Organo-montmorillonite · Organophilic clays · Oxidation

S. Yariv (✉) · I. Lapides
Institute of Chemistry, The Hebrew University of Jerusalem, Campus Edmund Y. Safra, 91904 Jerusalem, Israel
e-mail: yarivs@vms.huji.ac.il

M. Borisover
Institute of Soil, Water and Environmental Sciences, The Volcani Center, Agricultural Research Organization, POB 6, 50250 Bet Dagan, Israel

Introduction

Clay minerals are layered crystalline silicate minerals (phyllosilicates) [1] with chemically active surfaces rich with basic and acidic functional groups [2]. They are excellent adsorbing agents [3], and adsorption of organic compounds by clay minerals is widespread in nature and in industry. Complexes obtained by the adsorption of organic compounds by clay minerals are known as organoclays. In modern technology, organoclay-based nanocomposites obtained by modifying M-smectites (where M is an exchangeable cation) with long-chain cationic surfactants or with quaternary ammonium cations are potential candidates for serving as sorbents of different organic compounds, as thickeners in paints, greases, oil-base drilling mud, homogenizing fillers in the plastic industry and for the purpose of gelling of various organic liquids. They are also used in cleaning operations of drainage wastewater, oil-spill, and so on. This manuscript will summarize some of the basic knowledge on thermal analysis of organoclays and will review some of the recent studies carried out in our laboratory on organoclays which occur in the environment and of those applied in adsorption processes in the industry. Complexes in the environment or those which are used in industry are mainly those of the smectite clay mineral montmorillonite (MONT) and they will be treated here.

Each clay layer is composed of two types of sheets, tetrahedral and octahedral. In the tetrahedral sheet (labeled O), a continuous linkage of SiO_4 tetrahedra through sharing of three O atoms with three adjacent tetrahedra results with a planar network [1]. In the sheet, the tetrahedral silica groups are arranged in the form of a hexagonal network which is repeated indefinitely to form a phyllosilicate with the composition $[Si_4O_{10}]^{4-}$. A side view of the tetrahedral

sheet shows that it is composed of three parallel atomic planes, oxygens, silicones, and oxygens. The oxygens at the top of the tetrahedra form an open hexagonal network in this plane known as the clay-O-plane.

The octahedral sheet (labeled T) is obtained through condensation of single $[Al(OH)_6]^{3-}$ octahedra. Each O atom is shared by three octahedra, but two octahedra can share only two neighboring O atoms. In this sheet, the octahedral groups are arranged to form a hexagonal network, which is repeated indefinitely to form $[Al_4O_{12}]^{12-}$ sheet. A side view of the octahedral sheet shows that it is composed of a hexagonal plane Al atoms sandwiched between two dense hexagonal "OH planes". In MONT, only two thirds of the octahedra are filled with Al atoms [1].

A layer of MONT is composed of one octahedral sheet sandwiched between two tetrahedral sheets, condensed into one unit layer designated as "tetrahedral–octahedral–tetrahedral" (TOT) layer. In this unit layer, silica apices of one tetrahedral sheet are condensed with one of the OH plane of the octahedral sheet and the silica apices of a second tetrahedral sheet are condensed with the second OH plane of the octahedral sheet. A crystal of the mineral consists of TOT layers continuous in *a* and *b* directions, stacked one above the other in the *c* direction [1].

In MONT, some of the tetrahedral Si atoms are isomorphically substituted by Al, and some of the octahedral Al atoms are isomorphically substituted by Mg. The resulting charge deficiency is balanced by hydrated cations, mainly, Na, K, Mg, and Ca, of which more than 80% is located between parallel TOT layers. The space where these cations are located is named the interlayer space. In the interlayer, the cations are loosely held by electrostatic forces. They may be exchanged by inorganic and organic cations thus contributing to the MONT the property of being a cation exchanger. Water and polar organic molecules are attracted by the exchangeable cations and may intercalate between the layers causing the structure to expand in the direction perpendicular to the layers. This is the swelling property of MONT and is measured by basal spacing which is the distance between equivalent clay-O-planes of neighboring TOT layers. The thickness of the TOT layer is $\approx$0.96 nm. The thickness of the interlayer space is calculated by subtracting 0.96 nm from the basal spacing of the sample which is determined by X-ray diffraction. With intercalated water monolayer, the basal spacing of MONT is $\approx$1.26 nm [2].

Primary and secondary adsorption of organic compounds by montmorillonite

Organic ammonium cations are adsorbed by MONT by the mechanism of cation exchange in which inorganic exchangeable cations initially present in the interlayers are replaced by organic cations. For example, if Na-MONT is equilibrated with an aqueous solution of ethyl ammonium chloride, the following reaction occurs [3]:

$$C_2H_5NH_3Cl(aq) + Na - MONT(s) \leftrightarrow NaCl(aq) + C_2H_5NH_3 - MONT(s).$$

Organic cations in the interlayer space of MONT are also obtained by the adsorption of organic basic molecules followed by their protonation. Due to the polar effect of exchangeable cations on the adsorbed water in the interlayer, water molecules are acidic and may donate protons to organic bases. For example, adsorbed ethylamine is protonated in the interlayer as follows:

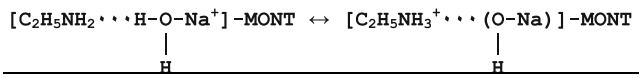

In addition to the long range electrostatic forces which hold the organic cations between the negatively charged clay layers, short range interactions, such as H-bonds between proton bearing organic cations and proton acceptor sites, e.g., oxygens of water or of the clay-O-plane [3] or coordination bonds between N and transition metal cations (e.g., Cu^{2+}) occur. With aromatic cations, π interactions may occur between the aromatic ring and the clay-O-plane [4]. Siloxane groups of the clay-O-plane are non-polar and may form van der Waals bonds with aliphatic chains. Contribution of van der Waals forces to the adsorption becomes significant with the size of the adsorbed cation.

Adsorptive properties of MONT for organic molecules are greatly modified by replacing native exchangeable metallic cations with organic ammonium cations and especially with long-chain or quaternary ammonium cations [5–8]. This replacement converts the clay into an organophilic substrate which is capable to adsorb polar and nonpolar organic molecules. Being widely applied in industry, the modified clays are commonly referred to as "organoclays." There are two types of organoclays: (i) those loaded with quaternary ammonium cations with one or two long alkyl chains and (ii) those loaded with small quaternary ammonium aliphatic and aromatic cations. The term "organophilic clays" is used for the former and "adsorptive clays" for the latter.

Primary adsorption is the loading of the clay with organic cations whereas secondary adsorption is the sorption of organic cations or molecules by the modified clays. The primary exchange of the metallic cation by long-chain organic ammonium cation is usually carried out in aqueous systems [9–16]. Driving force for this reaction is the

tendency of the hydrophobic organic tails to be drawn away from the aqueous system and the tendency of the inorganic cations to be fully hydrated in the aqueous system [3].

During the primary adsorption, the negative electric field induced by the clay surface is screened by the hydrophobic moiety of the organic cation and the ease of dehydration of organoclay increases [17]. Repulsive forces that occur between two similar double layers are thereby decreased, and when the loading of the clay is equal to its cation exchange capacity (CEC) the organoclay tends to coagulate. When cationic amines are in higher amounts than the CEC of the clay they are adsorbed in a secondary adsorption mechanism, providing positive charge to the layers. Again, there are repulsive forces between the layers of the oversaturated clay, and the organoclay saturated with excess ammonium cation tends to peptize. Aliphatic chains are consider as forming a bi-dimensional organic phase in a clay saturated with long-chain ammonium cations, where the clay-O-plane is screened by the nonpolar part of the organic cations [3].

Swelling of organoclays in organic liquids is used to determine organophilicity [18]. Gel formation results from secondary adsorption of molecules of the organic liquid into the interlayer of the organoclay. Gel volumes of a series of normal primary aliphatic ammonium montmorillonites in polar or non-polar liquids, such as nitrobenzene, benzene, and *iso*-amine alcohol show that the organophilicity is negligible until an ammonium cation with a chain of 10 carbon atoms is employed, and that at least 12 carbon atoms are required for gelation to occur [19].

The mechanism of the secondary adsorption by MONT loaded with long-chain ammonium cations (organophilic clays) differs from that in clay loaded with small quaternary ammonium cations (adsorptive clays). Adsorption efficiencies depend on several factors, such as size of the organic cation, porosity of the clay particle, the clay layer charge, size, and shape of the adsorbed molecule and the presence of water [20].

In adsorptive clay, the ammonium cations play the role of pillars, similar to their role in Al-pillared clay, holding the layers permanently apart without filling all the interlayer space, thus preserving the distance between the layers. Basal spacing of dehydrated MONT increases from 0.96 to 1.36 and 1.40 nm after primary adsorption of tetramethylammonium and tetraethylammonium cations, respectively. In the secondary adsorption of nonpolar molecules, which normally are not intercalated into the parent MONT, the nonpolar molecules penetrate into the expanded space between the pillars and the sorption capacity of the clay is greatly enhanced.

Thermal analysis of organo-clay complexes

Several thermal analysis methods are used in the study of thermal properties and processes of – complexes and of their fine structure. Among these techniques, the most common are differential thermal analysis (DTA) [21, 22, 23, 24], differential scanning calorimetry (DSC) [25], thermogravimetry (TG), evolved gas analysis (EGA) [26], thermo-IR-spectroscopy-analysis [27], and thermo-XRD-analysis [28].

In evolved gas analysis, the evolved gases during the thermal treatment pass either through a mass spectrometer, through an IR spectrophotometer [21], or through a gas titrimeter [22], where the evolved gases and their relative evolution with temperature are determined. If gases are evolved during a DTA study of a sample, then it is recommended to run a simultaneous DTA–EGA. This study supplies information on decomposition and oxidation products which are associated with the DTA peaks.

In thermo-IR-spectroscopy-analysis and thermo-XRD-analysis, the sample is heated at different temperatures, and IR spectra or X-ray diffractograms of the unheated and thermally treated samples are recorded. Changes in the IR spectra give information about changes in the fine structure of the complex occurring during the thermal treatment. Changes in the X-ray diffractograms give information about the effect of temperature on different crystallographic features of the sample (e.g., basal spacing).

Thermo-XRD-analysis combined with curve fitting calculations on the X-ray diffractograms supplies reliable information on the different organo-MONT or charcoal-MONT tactoids formed during the thermal treatment of an organo-MONT sample [28]. Curve fitting calculations result in one, two, three, or more peak components. Each of these components characterizes one type of tactoids. The tactoid (or oriented aggregate) is a cluster of parallel layers held by face-to-face interactions (FF associations). Thin layers of the adsorbed organic species with water molecules or of charcoal separate the TOT layers of the tactoid. These layers comprise the interlayer space of the clay mineral. According to Bragg's law, particles obtained from FF association of similar layers having similar interlayers, diffract X-ray. Location of the peak component maximum (in nm) describes the basal spacing of the respective tactoid. Relative peak component area (in percent from the total peak area) shows the relative concentration of the respective tactoid in the stack. The width of the peak component (in degree 2θ) represents the homogeneity of the respective tactoid in the stack. A homogeneous stack of tactoids poses a small component width whereas a non-homogeneous stack poses a broad width.

Thermal analysis of organo-clay complexes is carried out either under oxidizing environment (in air or under a flow of oxygen) or under a flow of an inert gas (such as nitrogen or argon). In DTA, oxidation of the adsorbed organic matter is recognized by significant exothermic peaks. Under inert atmospheres, desorption and pyrolysis of the organic matter occur giving rise to small DTA endothermic peaks. Most thermal analysis studies of organoclays were carried out in air atmosphere [24, 29].

Thermal analysis curves of DTA, DSC, TG, and EGA of MONT treated with N-bearing organic compounds, recorded either in oxidizing or inert atmosphere, can be divided into three regions: (i) region of the clay dehydration, (ii) region of the thermal reactions of the adsorbed organic matter, and (iii) region of the clay dehydroxylation where amorphous meta-clay becomes the principal inorganic phase. Reactions of the organic matter may continue in the temperature range of the third region together with the clay dehydroxylation [34]. First and third regions also exist in thermal analysis curves of the so called "normal" MONT which is not loaded by organic matter.

Water evolution from the clay is a thermal dissociation process. Bonds between adsorbed water molecules and acidic or basic sites on the internal and external surfaces of the clay dissociate due to heat supply. Dehydration shows an endothermic DTA peak, a heat absorption DSC peak, mass loss in TG curve, and EGA peak in H_2O evolution curve. Dehydration should not depend on whether it occurs in oxidizing or inert atmosphere. The thermal dehydration of the non-loaded clay and of the organoclay occurs in the same temperature range below 200–250 °C. However, in the presence of organic species in the interlayer, water structure is broken [2], and onset and peak maxima in thermal analysis curves of the organoclays may appear at lower temperatures than that in curves of the non-loaded MONT. In certain montmorillonites with tetrahedral substitutions of Si by Al, due to an increase of basic strength of the clay-O-plane [30], a very small loss of interlayer water may continue up to 400 °C [31].

Since some of the interlayer water is replaced by the adsorbed organic matter, size of dehydration peak is smaller in curves of organo-MONT than in curves of unloaded clay [18, 19]. Melting and boiling of non-adsorbed organic compounds adhered to the clay surface occur in this region giving rise to characteristic peaks in the thermal analysis curves. The appearance of such peaks in the first region is sometimes used to determine the presence of non-adsorbed organic matter in the clay mixture [32].

If the adsorbed organic matter has a high vapor pressure or a low boiling or sublimation point, part of it is sometimes evolved in the temperature range of the first region overlapping the water evolution. Evolution of organic matter in the first region cannot be detected from DTA, DSC, or TG curves but is detected from EGA curves [24].

Reactions occurring in the second region of the thermal analysis curves depend on whether the analysis is carried out in oxidizing or inert environment. In oxidizing atmosphere, the combustion of the organic matter commences at a temperature which is dependent on the activation energy of the oxidation. Exothermic DTA peaks and heat flow DSC peaks accompany this oxidation reaction. Evolution of H_2O, CO_2, and NO_2 and to some extent also NO and CO and other volatile oxidation and pyrolysis products is identified from EGA curves. Mass loss due to the escape of these gases is shown by a descent in the TG curve and peaks in the DTG curve [31, 33]. Depending on the nature of the adsorbed organic compound, the loading of the clay with the organic and the supply of oxygen, oxidation starts at 220–250 °C and it may continue up to 850 °C. The substrate clay serves as a catalyst for the oxidation, and the onset and peak temperatures differ from those recorded in curves of the neat organic matter.

In inert atmosphere volatilization, pyrolysis and cracking of the adsorbed organic matter occur [33]. For example, evolved gases in inert atmosphere in the second region of the thermal analysis of clays loaded with butylammonium are butylamine, NH_3, CH_4, and H_2 and very small amounts of propane, ethanol, acetic acid, and butane [34]. These reactions are endothermic. The intensity and resolution of the thermal analysis peaks are poor, and it is difficult to relate them to specific reactions.

The reactions occurring in the third region of the thermal analysis curves (above 500 °C) include the endothermic dehydroxylation of the clay [21–24]. This reaction is identified by an endothermic DTA peak, and an energy absorption DSC peak. According to the EGA clay, dehydroxylation leads to the evolution of H_2O formed from the hydroxyl groups of the octahedral sheets according to $OH^- + OH^- \leftrightarrow H_2O + \frac{1}{2}O_2$. Mass loss due to H_2O evolution is shown by a descent in the TG curve and a peak in the DTG curve. Dehydroxylation results in amorphous MONT are named as meta-montmorillonite. This is shown by a decrease in the intensity of characteristic X-ray peaks of MONT during thermo-XRD-analysis study of organoclays in the temperature range above 500 °C.

The peak minimum in the different thermal analysis curves of MONT due to the dehydroxylation depends on whether or not the clay is loaded with organic matter. In non-loaded "normal" MONT it appears at 680–710 °C but at lower temperatures when the clay is loaded with organic matter. This drop in peak temperature is associated with a reaction between the nascent water molecules and the interlayer charcoal which has been formed from the oxidation of the adsorbed organic matter during the second region of the thermal analysis curve. Chi Chou and McAtee

[35] ascribe this reaction to carbon oxidation but Shuali et al. [34] ascribe it to thermal hydrolysis.

A small S-shaped endothermic–exothermic peak system appears in the DTA curve of different montmorillonites at 850–980 °C. This system is not accompanied by mass loss, and it has been suggested that it is associated with the beginning of the crystallization of the amorphous meta-MONT into new phases [36].

Air-oxidation of adsorbed N-bearing organic compounds

The present section deals with the thermal air-oxidation of the organic component of the organoclay. Oxidation of most N-bearing organic compounds adsorbed onto MONT occurs in the second and third regions of the thermal analysis curve. Three oxidation steps are identified during the thermal treatment [21, 23, 24, 31]. The first oxidation step occurs between $\approx 235 \pm 15$ and $\approx 380 \pm 20$ °C. The second between $\approx 300 \pm 20$ and $\approx 560 \pm 15$ °C and the third in the temperature range of the third region of the thermal analysis curve, at temperatures above 500 °C. Each step is accompanied by an exothermic DTA peak, heat evolution DSC peak, mass loss in TG curve, and peak in DTG curve.

The nature of the thermal reactions depends on the amount of the organic matter which is present in the analysis cell and on the availability of oxygen along the thermal treatment. If the total amount of the organic compound in the thermal analyzed sample is small (e.g., a sample containing few mmol organic per 100 g clay) and the thermal analysis is carried out under a flow of oxygen the oxidation of H, C, and N to form H_2O, CO_2, and NO_2, respectively, is completed at a low temperature. No charcoal is formed, and there will be no organic matter to be oxidized in the third region of the thermal analysis curve. If this amount is high (few tens of mmol organic per 100 g clay) and the thermal analysis is carried out in air, in the first step the availability of oxygen is insufficient for a complete burning [37]. In this case, EGA shows that in the first oxidation step H_2O is the principal evolved gas obtained from the oxidation of the hydrogen component of the organic matter [38]. This water is termed "organic water". At this step only small amounts of CO_2 and NO_2 are detected by EGA [21, 23, 24]. Carbon and nitrogen atoms, which do not take part in the formation of the gaseous volatile oxides, form a black intercalated residue named ''charcoal'' [39] or ''petroleum coke'' [40].

The activity of organic matter inside the interlayer space during its transformation into charcoal is controlled by the stereoselectivity limitations that the interlayer space imposes on the orientation and packing arrangement of the organics. The charcoal in the interlayer space is composed of mono- or bi-layers of carbon atoms the structure of which is imposed by the parallel alumino-silicate layers [41].

Intercalation of adsorbed organic species into the interlayer space can be proven by thermo-XRD-analysis [28]. For this purpose, the unloaded and loaded samples are heated to temperatures above the irreversible dehydration of the clay, which depends on the exchangeable metallic cation [2], and are diffracted by X-ray. With no intercalated organic matter at this temperature, the clay collapses, and the basal spacing drops to ≈ 0.96 nm. In the presence of intercalated organic matter, charcoal is obtained at 235–380 °C, the clay does not collapse and spacings higher than 1.12 nm are obtained.

Low-temperature and high-temperature stable charcoal

The anionic dye Congo-red (CR) was adsorbed in considerable amounts by Na-, Cs-, Mg-, Al- and Fe-montmorillonites. The adsorption mechanism was of an acid–base type in which the clay supplied protons (from water hydrating the exchangeable cations) and certain functional groups on the CR anions were acting as proton acceptors [42]. Combined DTA–TG study of these dye-clay complexes showed three exothermic peaks of which the exact maximum locations depended on the exchangeable metallic cation [43]. The first exothermic peak at 316–357 °C was due to the first oxidation step in which organic water was evolved and intercalated charcoal was formed. A second exothermic peak at 490–530 °C represented the second oxidation step in which part of the charcoal was oxidized and the third peak at above 600 °C represented the third oxidation step due the oxidation of the rest of charcoal. From the relative areas and temperatures of the exothermic peaks and the relative mass loss in each thermal stage it was concluded that two different types of charcoal were obtained with different oxidation temperatures, giving exothermic peaks in the second and third regions of the thermal analysis curve, respectively. In accordance with their thermal stability they were named low-temperature- and high-temperature-stable charcoal (LTSC and HTSC, respectively). The exchangeable metallic cations determined the ratio between LTSC and HTSC. If the area of the exothermic peak is considered to be proportional to the amount of the charcoal that is oxidized, the ratio between LTSC and HTSC obtained in one DTA run can be calculated from the peak areas. With increasing acidity of the metallic cation, more HTSC and less LTSC were obtained. It was suggested that the high-temperature stable charcoal was obtained from the protonated positively charged

precursor, which formed π bonds with the clay-O-plane whereas the low-temperature stable charcoal was obtained from the negatively charged precursor, which did not form these π bonds [41]. Being negatively charged, CR should not form π bonds with the clay-O-plane unless it was protonated. With increasing surface acidity of the clay, more CR species were protonated.

The application of thermal analysis in mechanochemistry study is demonstrated by the following two examples. MONT complex of the cationic dye rhodamine 6G (R6G) was studied by combined DTA–EGA [44]. In this cation, phenyl is sterically constrained to be roughly perpendicular to the planar xanthene group. Although this dye is cationic, due to this steric hindrance π interactions between the clay-O-plane and R6G occur to a small extent only. The DTA curve of MONT treated with rhodamine 6G showed that most of the charcoal was oxidized before the dehydroxylation of the clay. A very small peak appeared in the CO_2 evolution curve above 600 °C indicating the presence of small amounts of HTSC in the interlayer space. DTA–TG curves of R6G-MONT obtained by mechanochemical adsorption in a dry system did not show any exothermic reaction above 600 °C, suggesting that the dye was located on the external surfaces of the clay [45].

MONT complex of the cationic dye crystal violet (CV) was obtained from an aqueous system [38] and by a dry mechanochemical adsorption [46]. The former was studied by combined DTA–EGA and the latter by DTA–TG. DTA–TG curves of CV-MONT obtained by the dry mechanochemical adsorption showed a very small exothermic peak at 620 °C, together with the dehydroxylation of the clay, associated with small amounts of mass loss up to 670 °C, suggesting that most of the adsorbed dye was located on the external surfaces of the clay. After washing the ground mixture with water, the DTA–TG curve showed a significant exothermic peak at 670 °C, together with considerable amounts of mass loss up to 770 °C, suggesting that the dye intercalated the clay. This curve was similar to the DTA–TG curve of CV-MONT obtained from an aqueous suspension. Thermo-XRD-analysis of unwashed and washed ground samples confirmed these observations. It appears that water is essential for the penetration of cationic dyes into the interlayer space of montmorillonite.

Thermo-XRD-analysis combined with curve fitting calculations on the different diffractograms of MONT complexes of the surfactant hexadecyltrimethylammonium (HDTMA) was recently studied (unpublished results). The thermal treatment was carried out up to 900 °C, and the diffractogram showed that at this temperature MONT became amorphous. Two types of HTSC-MONT tactoids were identified in this study and were labeled *a* and *b*. The thermo-XRD-analysis of the substrates was accompanied by TG, thermo-H-analysis, and thermo-C-analysis. At 150 °C only water was evolved. From 250 °C, three different types of tactoids of charcoal-MONT intercalation complexes were identified as follows: (1) at 250 and 360 °C tactoids of LTSC-MONT occurred with basal spacing 1.37–1.32 nm, (2) at 360, 420, and 550 °C tactoids of HTSC-*a*-MONT and of HTSC-*b*-MONT occurred with basal spacings 1.22–1.28 and 1.11–1.18 nm, respectively. After heating the organoclay at 700 °C, it was collapsed (0.96–1.03 nm) suggesting that after this treatment most of the clay was not intercalated by charcoal. From these spacings, it was suggested that in tactoids of LTSC-MONT monolayers of charcoal were lying in the interlayers parallel to the clay layers. In tactoids of HTSC-*a*-MONT monolayers of compacted charcoal were lying in the interlayers parallel to the clay layers. In tactoids of HTSC-*b*-MONT monolayers of compacted charcoal were lying in the interlayers parallel to the clay layers with carbon atoms keying into the ditrigonal holes of the clay-O-plane.

Aqueous sorption of nitrobenzene on Na-MONT and on two types of HDTMA-MONT was studied [47]. For this purpose, two types of the organo-montmorillonite were used in our adsorption studies. They were prepared by loading the clay with 41 and 90% of its CEC with HDTMA and were labeled OC-41 and OC-90, respectively. The substrates were heated 2 h in air at 150, 250, 360, and 420 °C. Mild heating of sorbents (at 150 °C) resulted in a distinct increase of the sorption efficacy probably associated with the escape of interlayer water. Treatment of organoclays at higher temperatures (250 and 360 °C) resulted in the first oxidation step of HDTMA and appearance of LTSC in the interlayer space. This had a little impact on the sorption efficacy as compared with organoclays treated at 150 °C. Further increase of the treatment temperature (420 °C) resulted in the transformation of LTSC into the HTSC (α and β varieties) and a decrease of a sorption efficacy of all sorbents. Mild heating of organoclays in air could be useful for improving their sorption potential.

Based on the data for LTSC-MONT and HTSC-MONT recorded during thermo-XRD-analysis of HDTMA-MONT the types of charcoal-MONT tactoids obtained in previous thermo-XRD-analysis studies before the use of curve fitting calculations are examined in the following paragraphs.

The secondary adsorption of nitrobenzene and *m*-nitrophenol by Na-MONT and by HDTMA-MONT were studied by thermo-XRD-analysis. Spacing of Na-clay non-loaded and loaded by nitrobenzene and *m*-nitrophenol before thermal treatment were 1.25, 1.23, and 1.27 nm, respectively. At 360 °C the non-loaded sample collapsed and the spacing dropped to 0.97 nm. Both loaded samples did not collapse, and spacing was 1.25 nm indicating the presence of HTSC-α. This is an indication that the adsorbed

nitrobenzene and *m*-nitrophenol were present in the interlayers of Na-MONT. Before the thermal treatment spacings of HDTMA-MONT non-loaded and after secondary adsorption of nitrobenzene and *m*-nitrophenol were 1.81, 1.78, and 2.02 nm, respectively. From these spacings, it is obvious that *m*-nitrophenol was intercalated but no clear information was obtained about location of nitrobenzene. Heating at 360 °C spacings of HDTMA-MONT non-loaded and treated with nitrobenzene and *m*-nitrophenol were 1.28, 1.24, and 1.26 nm, respectively showing that HTSC-α was formed in all the three samples. From this data, no unequivocal information was obtained on the location of the adsorbed molecules [48].

Urea–MONT complexes were obtained by grinding urea with different monoionic montmorillonites [49]. The swelling of the clay depended on the polarizing ability of the exchangeable cation. Cations with high polarizing ability (H^+, Al^{3+}, and Fe^{3+}) or medium polarizing ability (Li^+, Na^+, Mg^{2+}, Ca^{2+}, and Sr^{2+}) and transition-metal-cations (Co^{2+}, Ni^{2+}, and Cu^{2+}) led to an extensive swelling of the clay whereas cations with a low polarizing ability (K^+, Rb^+, Cs^+, NH_4^+, and Ba^{2+}) led to a limited swelling. There was a correlation between the thermal behavior of urea–clay intercalation complexes and the fine structure of the complexes at room temperature. With exchangeable cations with a high polarizability, the urea molecules were protonated at room temperature, and at 325 °C polymeric urea-condensation products (PUCP) were found in the interlayer space of tactoids with spacings of 1.28 nm similar to that of HTSC-*a* tactoids. At 375 °C, the basal spacing of the tactoids dropped to 1.11 indicating the presence of PUCP-tactoids similar to HTSC-*b* tactoids. With divalent exchangeable cations with a medium polarizing ability, at room temperature urea was bound to the cation via a water bridge. At 325 °C, PUCP were found in the interlayer space of tactoids with spacings of 1.30–1.37 nm similar to that of LTSC tactoids. At 375 °C, the spacing of the Mg-tactoids dropped to 1.13 indicating the presence of intercalated PUCP similar to that of HTSC-*b* but that of Ca- and Sr-tactoids dropped to 1.26 indicating the presence of intercalated PUCP similar to that of HTSC-*a*. With monovalent exchangeable cations, dehydration occurred at a relatively low temperature and the urea became directly coordinated to the cation. The cation-urea association protected the urea from thermal condensation. However, at 175–375 °C, urea completely evolved and the clay collapsed. With exchangeable transition-metal-cation, urea was directly coordinated to the cation. The cation–urea coordination complex protected the urea from thermal condensations. In the temperature range 175–375 °C urea gradually evaporated from the clay, and at 375 °C the clay collapsed.

The blue organo-clay color pigment (OCCP) naphthylazonaphthylammonium-MONT was synthesized from the white naphthylammonium-MONT by treating the latter with $NaNO_2$. Thermo-IR-spectroscopy analysis proved that the synthesized azo colorant was located in the interlayer space [50]. Recently, the thermo-XRD-analysis of naphthylazonaphthylammonium-MONT was compared with that of the precursor naphthylammonium-MONT [51, 52]. Samples were heated at 120–360 °C and diffracted by X-ray. The curve-fitted diffractogram of unheated naphthylammonium-MONT showed two peak-components with maxima at 1.35 and 1.58 nm with relative areas of 20 and 80% from the total peak-area, respectively, suggesting the presence of two types of tactoids, with monolayers of hydrated naphthylammonium cations lying parallel to the TOT clay layers and with naphthylammonium–naphthylamine associations probably tilted relative to the clay-O-layers, respectively. The thermo-XRD-analysis of naphthylammonium-MONT showed a collapse of most tactoids after 2 h at 120 °C (spacings <1.03 nm with relative peak areas of 84% and spacing 1.43 nm with relative area of 16%). A total collapse and complete loss of organic matter occurred at 180 °C, a temperature lower than that required for the boiling of naphthylamine.

The blue color pigment (OCCP) before heating exhibited two peak-components, at 1.28 and 1.50 nm, characterizing tactoids with monolayer and bilayer organic compounds in the interlayers, with relative peak-component areas of 74 and 26%, respectively. The 1.28 nm tactoids intercalated the azo dye. The decrease in basal spacing from 1.35 to 1.28 nm, as a result of the transformation of naphthylammonium into the azo dye, indicated stronger surface π interactions between the clay-O-planes and the azo dye than between these planes and naphthylammonium cations. Tactoids with bilayers organic compounds in the interlayers contained naphthylammonium, which probably did not react with $NaNO_2$ and was not transformed into the azo dye.

The thermo-XRD-analysis of naphthylazonaphthylamine-MONT showed different results when the heating occurred in stages or when the sample was directly heated at 360 °C. When the pigment was directly heated at 360 °C, most of the dye did not escape but became charcoal. During heating in stages, 73% of the azo dye decomposed at 180 °C, and tactoids became collapsed (0.96 nm). Some of the azo dye cations persisted in the interlayers of tactoids with spacing 1.22 nm (27%). At 300 and 360 °C, the organic cations were transformed to HTSC intercalating tactoids with spacings of 1.22–1.19 nm.

The microbial siderophore ferrioxamine B, produced by *Streptomyces* and *Nocardia* bacteria, is found in soil extracts. It belongs to the group of hydroxamate

siderophores. Iron carried by ferrioxamine B has been found to be an efficient source of Fe for many microorganisms as well as for a variety of plants. The Fe complex (FOB) obtains a wide, fairly flat configuration presenting a rather hydrophobic face, in contrast with the linear open chain with exposed active sites of the free ligand (desferrioxamine B, DFOB). The adsorption of FOB and DFOB by Ca-MONT from aqueous suspensions was investigated by thermo-XRD-analysis [53]. The initial spacings measured for unloaded Ca-MONT blank and Ca-MONT loaded with DFOB and FOB were 1.50, 1.43, and 1.75 nm, respectively. Upon heating the unloaded Ca-MONT collapsed at 250 and 360 °C to 1.00 and 0.97 nm, respectively. In contrast, spacings of sample loaded with DFOB upon heating at 250 and 360 °C became 1.32 and 1.28 nm, and those loaded with FOB became 1.37 and 1.22 nm, respectively. At 250 and 360 °C, the organic matter was converted into LTSC and HTSC-α, respectively, preventing the collapse of the clay, thus proving that DFOB and FOB penetrated into the interlayer space. At 25 °C, the folded FOB molecule caused an enlargement of the basal spacing from 1.50 (unloaded Ca-montmorillonite) to 1.75 nm. The total thickness of a FOB molecule is 0.55 nm. If the molecule was lying with its plane parallel to the clay layers, one would expect a basal spacing of 1.50–1.55 nm. The measured basal spacing of 1.75 nm, which decreased to 1.70 nm after the dehydration of the clay at 120 °C, suggested that the adsorbed FOB was lying slightly tilted within the clay layers. After thermal dehydration at 120 °C, the basal spacing decreased to 1.38 nm. Since the van der Waals diameter of C is 0.35 nm, this basal spacing suggests that the adsorbed DFOB formed a monolayer, lying almost parallel to the silicate layer.

The adsorption of the cationic alkaloid berberine by MONT took place by two types of adsorption mechanism: (1) cation exchange and (2) secondary organophilic adsorption [54]. Thermo-XRD-analysis proved that the adsorbed berberine was located in the interlayer space. With a low loading (up to 15 mmol of berberine per 100 g clay) a basal spacing of 1.28–1.30 nm characterized monolayers of berberine parallel to the clay-O-planes. With a high loading (≥55 mmol of berberine per 100 g clay) a basal spacing of 1.59 nm characterized bilayers of berberine parallel to the clay-O-planes. With a very high loading (≥100 mmol of berberine per 100 g clay) a basal spacing of 1.66 nm, obtained after heating at 190 °C, characterized berberine tilted relative to the clay-O-planes of the TOT skeletons. At 360 °C, spacing of this sample dropped to 1.47 nm but at 420 °C it dropped to 1.27 nm, suggesting the presence of LTSC and HTSC-α, respectively, whereas samples with <100 mmol berberine showed the latter spacing already after heating at 360 °C.

The adsorption of protonated Congo-red (HCR) by MONT was investigated by thermo-XRD-analysis [55] and by thermo-visible-spectroscopy-analysis [56]. MONT was loaded at pH 1 with increasing amounts of CR up to 75 mmol per 100 g clay. Diffractograms of samples treated at 420 °C showed broad peaks and were curve-fitted to determine basal spacings of the different tactoids. The broad peak of one sample may contain up to four components. Component A with a maximum at 0.95–1.01 nm characterized tactoids with collapsed interlayers. Component B at 1.01–1.07 nm characterized tactoids with a non-complete collapse due to the presence of hydroxy-cations such as $[Ca(OH)]^+$ in the interlayers which are too large for a complete keying in the ditrigonal holes of the clay-O-planes. Component C at 1.12–1.31 nm characterized tactoids with intercalated planar monolayers of charcoal (LTSC, HTSC-α, and HTSC-β). In the presence of high amounts of adsorbed organic matter, components A and B converged whereas component C split into two sub-components C_1 and C_2, with maxima at ≈1.12 and ≈1.26 nm, respectively. The latter spacing represented tactoids with intercalated compacted monolayer charcoal with no keying (HTSC-α) whereas the former represented tactoids with intercalated charcoal monolayers with carbon atoms keying into the ditrigonal holes of the oxygen plane (HTSC-β). Component D at ≈1.60 nm characterized tactoids with expanded interlayers containing intercalated charcoal of multi-layer carbon. The presence of components C and D in the curve-fitted diffractograms proved that before the thermal treatment the adsorbed HCR was located inside the interlayer space of the smectite. Depending on the amount of adsorbed CR, three types of diffractograms were identified. With small adsorption components A, B, and C were detected. With higher adsorption components A, B, C, and D were detected, and with very high adsorption, components A, C_1, C_2, and D were obtained.

Gemini surfactants were obtained by refluxing the *bis*(2-bromoethyl) ether with *N*–*n*,alkyl-*N*,*N*-dimethylamine in *iso*-propanol. Recently, the thermogravimetric analyses (combined TG and DTG analyses) of Na-MONT intercalated with several Gemini surfactants and of MONT modified by cetyltrimethyl ammonium bromide (CTAB) were investigated [57]. The analyses showed four-step degradation which corresponds to residual water desorption, dehydration followed by decomposition of the adsorbed organic compound, and the dehydroxylation of the clay.

Recently, the secondary adsorption of stearic acid by dodecyltrimethyl ammonium-MONT (DDTA-MONT) was investigated by combined TG and DTG analyses [58]. Curves of Ca-MONT and of DDTA-MONT, both loaded with stearic acid were recorded. Stearic acid volatilizes at 179 °C but when is adsorbed onto the interlayer of

Ca-MONT it sublimes at 248 °C and onto the interlayer of DDTA-MONT it sublimes at 322 °C. The surfactant sublimes at 208 °C but when is adsorbed onto the interlayer of MONT it sublimes at 375 °C.

Conclusions

This review demonstrates that using simultaneously different thermal analysis methods one can get the information on the fine structure of the organo-clay complexes.

Future trends

From this short review it appears that in the next future we are going to see more and more simultaneous DTA–EGA studies of organoclays. Very little is known about the structure and properties of the different charcoal-clay tactoids. More information is required in order that these nanocomposite materials will be applied in modern technologies.

Acknowledgements This research was supported by a grant from the Israeli Science Foundation (No. 919.08) and by a grant from the Ministry of Science, Culture and Sport and the Ministry of Research (Infrastructure 3-4136).

References

1. Yariv S, Michaelian KH. Structure and surface acidity of clay minerals. In: Yariv S, Cross H, editors. Organo-clay complexes and interactions. New York: Marcel Dekker; 2002. p. 1–38.
2. Yariv S. Wettability of clay minerals. In: Schrader ME, Loeb G, editors. Modern approach to wettability. New York: Plenum Press; 1992. p. 279–326.
3. Yariv S. Introduction to organo-clay complexes and interactions. In: Yariv S, Cross H, editors. Organo-clay complexes and interactions. New York: Marcel Dekker; 2002. p. 39–111.
4. Yariv S. Staining of clay minerals and visible absorption spectroscopy of dye–clay complexes. In: Yariv S, Cross H, editors. Organo-clay complexes and interactions. New York: Marcel Dekker; 2002. p. 463–566.
5. Chun Y, Sheng GY, Boyd SA. Sorptive characteristics of tetraalkylammonium-exchanged smectite clays. Clay Clay Miner. 2003;51:451–8.
6. Boyd SA, Chiou CT, Mortland MM. Sorption characteristics of organic compounds on hexadecyltrimethylammoniumsmectite. Soil Sci Soc Am J. 1988;52:652–60.
7. Boyd SA, Jaynes WF, Ross BS. Immobilization of organic contaminants by organo-clays. Application to soil restoration and hazardous waste containment. In: Baker RS, editor. Organic substances and sediments in water. Chelsea: Lewis Publishers; 1991. p. 181–200.
8. Giese RF, van Oss CJ. Organophilicity and hydrophobicity of organoclays. In: Yariv S, Cross H, editors. Organo-clay complexes and interactions. New York: Marcel Dekker; 2002. p. 175–91.
9. Mortland MM, Shaobai S, Boyd SA. Clay-organic complexes as adsorbents for phenol and chlorophenol. Clays Clay Miner. 1986;34:581–5.
10. Sheng GY, Shihe Xu, Boyd SA. Mechanisms controlling sorption of neutral organic contaminants by surfactant-derived and natural organic matter. Environ Sci Technol. 1996;30:1553–60.
11. Sheng GY, Shihe Xu, Boyd SA. Surface heterogeneity of trimethylphenylammonium-smectite as revealed by adsorption of aromatic hydrocarbons from water. Clays Clay Miner. 1997;45: 659–68.
12. Sheng GY, Boyd SA. Polarity effect on dichlorobenzene sorption by hexadecyltrimethylammonium exchanged clays. Clays Clay Miner. 2000;48:43–50.
13. Hermosin MC, Cornejo J. Binding mechanism of 2,4-dichlorophenoxyacetic acid by organo-clays. J Environ Qual. 1993;22: 325–32.
14. Hermosin MC, Crabb A, Cornejo J. Sorption capacity of organoclays for anionic and polar organic contaminants. Fresenius Environ Bull. 1995;4:514–21.
15. He H, Ding Z, Zhu J, Yuan P, Xi Y, Yang D, Frost RL. Thermal characterization of surfactant-modified montmorillonite. Clays Clay Miner. 2005;53:287–93.
16. Xi Y, Frost RL, He H. Modification of the surfaces of Wyoming montmorillonite by the cationic surfactants alkyl trimethyl, dialkyl dimethyl, and trialkylmethyl ammonium bromides, J. Colloids Interface Sci. 2007;305:150–8.
17. Yariv S. Organophilic pores as proposed primary migration media for hydrocarbons in argillaceous rocks. Clay Sci. 1976;5: 19–29.
18. Jordan JW. Organophilic bentonites I. Swelling in organic liquids. J Phys Colloid Chem. 1949;53:294–306.
19. Jordan JW. Alteration of the properties of bentonite by reactions with amines. Mineral Mag. 1949;28:598–605.
20. Barrer RM. Shape selective sorbents based on clay minerals—a review. Clays Clay Miner. 1989;37:385–95.
21. Langier-Kuzniarowa A. Thermal analysis of organo-clay complexes. In: Yariv S, Cross H, editors. Organo-clay complexes and interactions. New York: Marcel Dekker; 2002. p. 273–344.
22. Paulik F. Special trends in thermal analysis. Chichester: Willey; 1995.
23. Yariv S. Differential thermal analysis (DTA) of organo-clay complexes. In: Smykatz-Kloss W, SStJ Warne, editors. Lecture notes in earth sciences 38. Thermal analysis in the geosciences. Berlin: Springer; 1991. p. 328–51.
24. Yariv S. Differential thermal ananlysis (DTA) in the study of thermal reactions of organo-clay complexes. In: Ikan R, editor. Natural and laboratory simulated thermal geochemical processes. Dordrecht: Kluver Academic Publishers; 2003. p. 253–96.
25. Yariv S, Ovadyahu D, Nasser A, Shuali U, Lahav N. Thermal analysis study of heat of dehydration of tributyl-ammonium smectites. Thermochim Acta. 1992;207:103–13.
26. Yariv S. Combined DTA-mass spectroscopy of organo-clay complexes. J Therm Anal. 1990;36:1953–61.
27. Yariv S. IR spectroscopy and thermo-IR spectroscopy in the study of organo-clay complexes. In: Yariv S, Cross H, editors. Organo-clay complexes and interactions. New York: Marcel Dekker; 2002. p. 345–462.
28. Yariv S, Lapides I. The use of thermo-XRD-analysis in the study of organo-smectite complexes. J Therm Anal Calorim. 2005;80: 11–26.
29. Cebulak S, Langier-Kuzniarowa A. Some remarks on methodology of thermal analysis of clay minerals. J Therm Anal Calorim. 1998;53:375–81.
30. Yariv S. The effect of tetrahedral substitution of Si by Al on the surface acidity of the oxygen plane of clay minerals. Intern Rev Phys Chem. 1992;11:345–75.

31. Ovadyahu D, Lapides I, Yariv S. Thermal analysis of tributylammonium montmorillonite and Laponite. J Therm Anal Calorim. 2007;87:125–34.
32. Ovadyahu D, Yariv S, Lapides I. Mechanochemical adsorption of phenol by TOT swelling clay minerals: I. Thermo-IR-spectroscopy and X-ray study. J Therm Anal Calorim. 1998;51:415–30.
33. Yariv S. Study of the adsorption of organic molecules on clay minerals by differential thermal analysis. Thermochim Acta. 1985;88:49–68.
34. Shuali U, Steinberg M, Yariv S, Mueller Vonmoos M, Kahr G, Rub A. Thermal analysis of sepiolite and palygorskite treated with butylamine. Clay Miner. 1990;25:107–19.
35. Chi Chou C, McAtee JL. Thermal decomposition of organo-ammonium compounds exchanged onto montmorillonite and hectorite. Clays Clay Miner. 1969;17:339–46.
36. Mackenzie RC. Simple phyllosilicates based on gibbsite- and brucite-like sheets. In: Mackenzie RC, editor. Differential thermal analysis. London: Academic Press; 1970. p. 497–537.
37. Bodenheimer W, Heller L, Yariv S. Organo-metallic clay complexes: VII. Thermal analysis of montmorillonite-diamine and glycol complexes. Clay Miner. 1966;6:167–77.
38. Yariv S, Mueller-Vonmoos M, Kahr G, Rub A. Thermal analytical study of the adsorption of crystal violet by montmorillonite. Thermochim Acta. 1989;148:457–66.
39. Allaway WH. Differential thermal analysis of clays treated with organic cations as an aid in the study of soil colloids. Soil Sci Am Proc. 1949;13:183–8.
40. Bradley WF, Grim RE. Colloid properties of layer silicates. J Phys Chem. 1948;52:1404–13.
41. Yariv S. The role of charcoal on DTA curves of organo-clay complexes. An overview. Appl Clay Sci. 2004;24:225–36.
42. Yermiyahu Z, Lapides I, Yariv S. Visible absorption spectroscopy study of the adsorption of Congo-red by montmorillonite. Clay Miner. 2003;38:483–500.
43. Yermiyahu Z, Landau A, Zaban A, Lapides I, Yariv S. Monoionic montmorillonites treated with Congo-red Differential thermal analysis study. J Therm Anal Calorim. 2003;72:431–41.
44. Yariv S, Kahr G, Rub A. Thermal analysis of the adsorption of rhodamine 6G by smectite minerals. Thermochim Acta. 1988; 135:299–306.
45. Landau A, Zaban A, Lapides I, Yariv S. Montmorillonite treated with rhodamine-6G mechanochemically and in aqueous suspensions-simultaneous DTA–TG study. J Therm Anal Calorim. 2002;70:103–13.
46. Lapides I, Yariv S, Golodnitsky D. Simultaneous DTA–TG study of montmorillonite mechanochemically treated with crystal-violet. J Therm Anal Calorim. 2002;67:99–112.
47. Borisover M, Bukhanovsky N, Lapides S, Yariv S. Thermal treatment of organoclays: effect on the aqueous sorption of nitrobenzene on *n*-hexadecyltrimethyl ammonium montmorillonite. Appl Surf Sci. 2010;256:5539–44.
48. Burstein F, Borisover M, Lapides S, Yariv S. Secondary adsorption on nitrobenzene and *m*-nitrophenol by hexadecyltrimethylammonium-montmorillonite: thermo-XRD-analysis. J Therm Anal Calorim. 2008;92:35–42.
49. Abramova E, Lapides I, Yariv S. Thermo-XRD investigation of monoionic montmorillonites mechanochemically treated with urea. J Therm Anal Calorim. 2007;90:97–106.
50. Yermiyahu Z, Lapides I, Yariv S. Thermo-infrared-spectroscopy analysis of the interaction of naphthylammonium-montmorillonite with sodium nitrite. Colloid Polym Sci. 2008;286:1233–42.
51. Yermiyahu Z, Lapides I, Yariv S. Synthesis and thermo-XRD-analysis of the organo-clay color pigment Naphthylazonaphthylammonium-montmorillonite. J Therm Anal Calorim. 2007; 88:795–800.
52. Yermiyahu Z, Kogan A, Lapides I, Pelly I, Yariv S. Thermal study of naphthylammonium- and naphthylazonaphthylammonium montmorillonite, XRD and DTA. J Therm Anal Calorim. 2008;91:125–35.
53. Siebner-Freibach H, Hadar Y, Yariv S, Lapides I, Chen Y. Thermospectroscopic study of the adsorption mechanism of the hydroxamic siderophore ferrioxamine B by calcium montmorillonite. J Agric Food Chem. 2006;54:1399–408.
54. Cohen E, Joseph T, Lapides I, Yariv S. The adsorption of berberine by montmorillonite and thermo-XRD analysis of the organo-clay complex. Clay Miner. 2005;40:223–32.
55. Yermiyahu Z, Lapides I, Yariv S. Thermo-XRD-analysis of montmorillonite treated with protonated Congo-red. Curve fitting. Appl Clay Sci. 2005;30:33–41.
56. Yermiyahu Z, Lapides I, Yariv S. Thermo-visible-absorption-spectroscopy study of the protonated Congo-red montmorillonite complex. Appl Clay Sci. 2007;37:1–11.
57. Ni R, Huang Y, Yao C. Thermogravimetric analysis of organoclays intercalated with the Gemini surfactants. J Therm Anal Calorim. 2009;96:943–7.
58. Lu L, Cai J, Frost RL. Desorption of stearic acid upon surfactant adsorbed montmorillonite. J Therm Anal Calorim. 2010;100: 141–4.